

Three-Dimensional Photonic Crystal Composites with High Refractive Index Thin Films

Mike P. C. Taverne¹, Xu Zheng¹, Yu-Shao Jacky Chen¹, Katrina A. Morgan², Lifeng Chen¹, GhadahAlzaidy², Chung-Che Huang², Ying -Lung Daniel Ho^{1,3}, Daniel W. Hewak², and John G. Rarity¹

¹Department of Electrical and Electronic Engineering, University of Bristol, Bristol, UK

²Optoelectronics Research Centre, University of Southampton, Southampton, UK

³Department of Mathematics, Physics & Electrical Engineering, Northumbria University, Newcastle upon Tyne, UK

*corresponding author, E-mail: Mike.Taverne@bristol.ac.uk

Abstract

We study polymer photonic crystals coated with varying thickness of high refractive index material aiming to make functional photonic devices capable of controlling light through band structure and dispersion. We observed red shifts of partial bandgaps in the near infrared region when the thickness of deposited MoS₂ films increases. A ~150 nm red shift of the fundamental and high order bandgaps is measured after a ~15nm thick MoS₂ coating.

1. Introduction

High refractive index contrast photonic crystals show bandgaps blocking light propagation in all directions. Starting from a low index template and depositing high index material, we can open and enlarge bandgaps and control the dispersion. Here, such refractive index composites are fabricated by coating polymer three-dimensional (3D) woodpile structures (see Figure 1) with thin molybdenum disulphide (MoS₂) films. A two-step process is used: 3D polymer woodpile templates are fabricated by a direct laser writing (DLW) method followed by chemical vapour deposition (CVD) of MoS₂ [1]. The optical properties of the composite structures are examined by measuring reflection spectra changes after each 2 nm thin film coating via our angle-resolved Fourier imaging spectroscopy (FIS) system [2-4].

2. Fabrication

A direct laser writing (DLW) system based on the two-photon polymerization (2PP) method is used to fabricate woodpile photonic crystals in a photoresist (IP-L) [2]. The laser beam is produced by a femtosecond fibre laser and the beam is focused through an oil-immersion objective lens with an NA of 1.4 and 100× magnification into the photoresist. Figure 1 (a)-(c) illustrates the thin film coating of these woodpile templates and (d) shows an SEM image of the fabricated woodpile template. The dimensions of the fabricated body-centered cubic (BCC) woodpile [5,6] are vertical period c and lateral rod distance a , $c = a = 1\mu\text{m}$, rod height $h \sim 580$ nm, rod width $w \sim 240$ nm. The sides of the structure are open, ensuring that the gas flow can get in providing even coatings. The lattice constant c is chosen to give a starting bandgap around $1.2\text{-}4\ \mu\text{m}$ so that it moves

into the $1.5\text{-}1.6\mu\text{m}$ range after high refractive index material deposition.

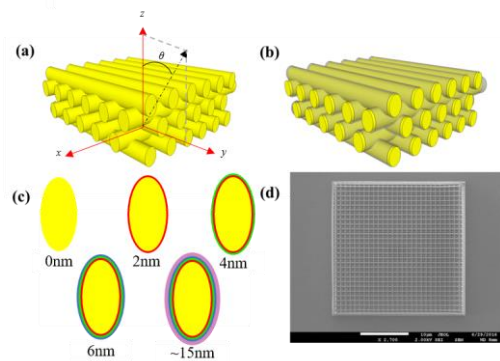


Figure 1: Schematics of (a) non-coated woodpile template (b) thin film MoS₂-coated woodpile template (c) resulting rod cross section after each 1nm MoS₂ thin film coated. Colours (red, green and blue) are used to indicate the 1nm thin films coated in sequence. (d) SEM scanning image of the fabricated woodpile template.

We perform chemical vapour deposition (CVD) of MoS₂ thin film on our fabricated polymer woodpile templates to achieve high refractive index contrast composites. Thin film deposition for 30 mins at room temperature followed by annealing treatment at 250° C for 3 hours achieves a ~2 nm MoS₂ deposition while avoiding any obvious thermal deformation of woodpile templates.

3. Simulation and Measurement Results

To visualize the modification of the photonic band-structures, angle-resolved reflection spectra after each thin film deposition are measured via our angle-resolved Fourier imaging spectroscopy (FIS) system [2-4]. Figure 2 plots the measured angle-resolved reflection spectra for bcc woodpile structures with varying MoS₂ thickness (0-15nm). The angles in Figure 2 correspond to the collection angle θ relative to the Z direction, in the YZ plane (See Figure 1(a)). Photonic band calculations for the corresponding directions were also done using the following refractive index values: $n(\text{IP-L})=1.52$ and $n(\text{MoS}_2)=3.1$.

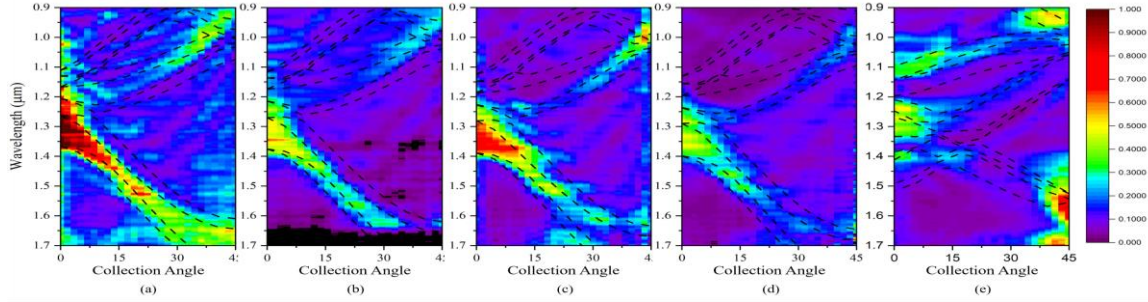


Figure 2: Measured angle-resolved reflection spectra of woodpile structures (a) non-coated (b) 2nm (c) 4nm (d) 6nm (e) 15 nm MoS₂ thin film coated. Dashed lines indicate their corresponding photonic band structures calculated via PWE method.

4. Discussion

Figure 3a shows the measured spectra at normal incidence (solid lines) and simulated results using the PWE method. The simulations show (figure 3b) a 6 nm red shift of the fundamental bandgap (at $\sim 1.3 \mu\text{m}$) at normal incidence after the first 2 nm MoS₂ thin film coating (red dashed line), followed by another 12 nm and 14 nm red shift after the second (green dashed line), and the third deposition (blue dashed line). For the measurement, a clear red shift of the lower edge of the bandgap after the first (~ 10 nm, red solid line) and second (~ 12 nm, green solid line) deposition can be observed. However, the red shift after the third deposition (blue solid line) is not obvious. To have more easily observable shift, we coated $\sim 15\text{nm}$ MoS₂ film onto a bare template. The red shift between non-coated and 15 nm coated is around 150 nm which is relatively large compared to previous data. The result is presented in Figure 3 (a), purple solid line for measurement and dash line for PWE simulation.

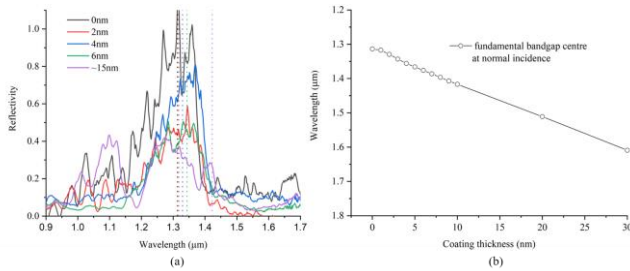


Figure 3: (a) comparison of the normal incidence spectrum for different coating thicknesses with the corresponding simulation bandgap positions in vertical dashed lines. (b) the simulated bandgap position as a function of coating thickness.

5. Conclusions

Polymer woodpile templates are fabricated, and we managed to measure partial bandgaps at near infrared region. We observed a ~ 10 nm red shift of bandgaps after each 2 nm MoS₂ thin film deposition and $\sim 1.3 \mu\text{m}$ red shift for the ~ 15 nm MoS₂ coated. Simulation results also show red shifts of bandgaps with increasing deposition thickness and optimized gap-midgap ratio. By measuring the red shifts of bandgaps, one can determine the thickness of depositions via comparing with calculations. Thus, this

optical method can also work as an alternative way to measure the thickness of deposited films without contacting or damaging the films.

Acknowledgements

This work was carried out using the computational facilities of the Advanced Computing Research Centre, University of Bristol, Bristol, UK and funded by the Engineering and Physical Sciences Research Council (EPSRC) grant EP/M009033/1 and EP/M024458/1.

References

- [1] C.-C. Huang, F. Al-Saab, Y. Wang, J.-Y. Ou, J.C. Walker, S. Wang, B. Gholipour, R.E. Simpson, D.W. Hewak, Scalable high-mobility MoS₂ thin films fabricated by an atmospheric pressure chemical vapor deposition process at ambient temperature, *Nanoscale*, 6:12792–12797, 2014.
- [2] L.-F. Chen, K. Morgan, G. Alzaidy, C-C Huang, Y. -L. Daniel Ho, Mike P. C. Taverne, X. Zheng, Z. Ren, Daniel W. Hewak, John G. Rarity, Observation of Complete Photonic Bandgap in Low Refractive Index Contrast Inverse Rod-Connected Diamond Structured Chalcogenides, *ACS Photonics* 6:1248–1254, 2019.
- [3] L.-F. Chen, M. Lopez-Garcia, M. P. C. Taverne, X. Zheng, J.-D. Lin, Y.-L. D. Ho, J. G. Rarity, Direct Wide-angle Measurement of Photonic Bandstructure in a Three-dimensional Photonic Crystal using Infrared Fourier Imaging Spectroscopy, *Opt. Lett.* 42:1584-1587, 2017.
- [4] L.-F. Chen, M. P. C. Taverne, X. Zheng, J.-D. Lin, R. Oulton, M. Lopez-Garcia, Y.-L. D. Ho, J. G. Rarity, Evidence of Near-Infrared Partial Photonic Bandgap in Polymeric Rod-connected Diamond Structure, *Opt. Express* 23:26565-26575, 2015.
- [5] X. Zheng, M. P. C. Taverne, Y.-L. D. Ho, J. G. Rarity, Cavity Design in Woodpile Based 3D Photonic Crystal, *Appl. Sci.* 8:1087, 2018.
- [6] I. Staude, G. von Freymann, S. Essig, K. Busch, and M. Wegener, Waveguides in three-dimensional photonic-bandgap materials by direct laser writing and silicon double inversion, *Opt. Lett.* 36:67-69, 2011.